

Approximating the Perfect Sampling Grids for Computing the Eigenvalues of Toeplitz-like Matrices Using the Spectral Symbol

Sven-Erik Ekström

see@2pi.se

Athens University of Economics and Business

December 20, 2024

Abstract

In a series of papers the author and others have studied an asymptotic expansion of the errors of the eigenvalue approximation, using the spectral symbol, in connection with Toeplitz (and Toeplitz-like) matrices, that is, $E_{j,n}$ in $\lambda_j(A_n) = f(\theta_{j,n}) + E_{j,n}$, $A_n = T_n(f)$, f real-valued cosine polynomial. In this paper we instead study an asymptotic expansion of the errors of the equispaced sampling grids $\theta_{j,n}$, compared to the exact grids $\xi_{j,n}$ (where $\lambda_j(A_n) = f(\xi_{j,n})$), that is, $E_{j,n}$ in $\xi_{j,n} = \theta_{j,n} + E_{j,n}$. We present an algorithm to approximate the expansion. Finally we show numerically that this type of expansion works for various kind of Toeplitz-like matrices (Toeplitz, preconditioned Toeplitz, low-rank corrections of them). We critically discuss several specific examples and we demonstrate the superior numerical behavior of the present approach with respect to the previous ones.

1 Introduction

For a given banded Hermitian Toeplitz matrix, $T_n(f) \in \mathbb{R}^{n \times n}$,

$$T_n(f) = \begin{bmatrix} \hat{f}_0 & \cdots & \hat{f}_m & & \\ \vdots & \ddots & & \ddots & \\ \hat{f}_m & & \ddots & & \\ & \ddots & & \ddots & \hat{f}_m \\ & & \ddots & \ddots & \vdots \\ & & & \hat{f}_m & \cdots & \hat{f}_0 \end{bmatrix}$$

we can easily associate a real-valued spectral symbol f , independent of n , namely

$$f(\theta) = \sum_{k=-n}^n \hat{f}_k e^{ik\theta} = \sum_{k=-m}^m \hat{f}_k e^{ik\theta} = \hat{f}_0 + 2 \sum_{k=0}^m \hat{f}_k \cos(\theta),$$

and note that \hat{f}_k are the Fourier coefficients of $f(\theta)$, that is,

$$\hat{f}_k = \frac{1}{2\pi} \int_{-\pi}^{\pi} f(\theta) e^{-ik\theta} d\theta.$$

We say that the symbol f generates the Toeplitz matrix of order n when $T_n(f)$ is defined as $[\hat{f}_{i-j}]_{i,j=1}^n$. The eigenvalues of $T_n(f)$, denoted $\lambda_j(T_n(f))$, can be approximated by sampling the symbol f with an equispaced grid $\theta_{j,n}$, that is,

$$\lambda_j(T_n(f)) = f(\theta_{j,n}) + E_{j,n}^{\lambda,\theta} \quad (1)$$

where we typically use the following standard equispaced grid

$$\theta_{j,n} = \frac{j\pi}{n+1} = j\pi h, \quad j = 1, \dots, n, \quad h = \frac{1}{n+1}, \quad (2)$$

and the error, for grid $\theta_{j,n}$, is $E_{j,n}^{\lambda,\theta} = \mathcal{O}(h)$; see for example [7, 14].

In a series of papers [4, 5, 6] an asymptotic expansion of the error $E_{j,n}^\theta$ in (1),

$$E_{j,n}^{\lambda,\theta} = \sum_{k=1}^{\alpha} c_k(\theta) h^k + E_{j,n,\alpha}^{\lambda,\theta} \quad (3)$$

was studied. In [12] an algorithm to approximate the functions $c_k(\theta)$, in the grid points θ_{j,n_1} for a chosen n_1 , was proposed: such an approximation is denoted by $\tilde{c}_k(\theta_{j,n_1})$, for $k = 1, \dots, \alpha$ and α chosen properly. We thus have

$$\begin{aligned} E_{j,n_1}^{\lambda,\theta} &= \sum_{k=1}^{\alpha} c_k(\theta_{j,n_1}) h^k + E_{j,n_1,\alpha}^{\lambda,\theta} \\ &= \sum_{k=1}^{\alpha} \tilde{c}_k(\theta_{j,n_1}) h^k + \tilde{E}_{j,n_1,\alpha}^{\lambda,\theta}. \end{aligned}$$

Ignoring the error term $\tilde{E}_{j,n_1,\alpha}^{\lambda,\theta}$, we obtain the following expression to approximate the eigenvalues of a generated matrix $T_{n_m}(f)$ with indices $j_m = 2^{m-1} j_1$ (where $j_1 = \{1, \dots, n\}$), that is

$$\lambda_{j_m}(T_{n_m}(f)) \approx \tilde{\lambda}_{j_m}^{(\alpha)}(T_{n_m}(f)) = f(\theta_{j,n_1}) + \sum_{k=1}^{\alpha} \tilde{c}_k(\theta_{j,n_1}) h_m^k,$$

where $n_m = 2^{m-1}(n_1 + 1) - 1$. In Figure 1 we show three grids, given by $n_k = 2^{k-1}(n_1 + 1) - 1$, namely $n_1 = 3, n_2 = 7$, and $n_4 = 31$. Blue circles indicate the sets of indices j_k such that θ_{j_k, n_k} always are the same for any k .

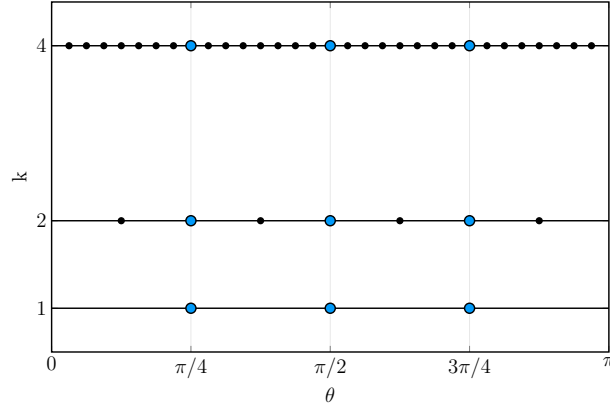


Figure 1: Three grids θ_{j,n_k} with $k = 1, 2, 4$, $n_k = 2^{k-1}(n_1 + 1) - 1$, and $n_1 = 3$. The subgrids θ_{j_k, n_k} , which is the same for any k , is indicated by blue circles ($j_k = 2^{k-1} j_1$, $j_1 = \{1, \dots, n_1\}$).

If we use the interpolation–extrapolation scheme introduced in [11], then we can approximate $\tilde{c}_k(\theta_{j,n})$ for any n and thus we can compute numerically the full spectrum of $T_n(f)$ by

$$\lambda_j(T_n(f)) \approx \tilde{\lambda}_j^{(\theta,\alpha)}(T_n(f)) = f(\theta_{j,n}) + \sum_{k=1}^{\alpha} \tilde{c}_k(\theta_{j,n}) h^k. \quad (4)$$

Note that the procedure using the asymptotic expansion (4) also works for more general types of Toeplitz-like matrices, for example for preconditioned Toeplitz matrices [2], and block-Toeplitz matrices generated by matrix-valued symbols [10], and even in a differential setting when considering the isogeometric approximation of the Laplacian eigenvalue problem in any dimension [9]. The latter example is quite important since the involved matrices can be written as low-rank corrections of either of Toeplitz or of preconditioned Toeplitz matrices. We call this type of methods *matrix-less* since they do not need to construct a matrix, of arbitrary order n , to approximate its eigenvalues (after the initial step when approximating $c_k(\theta_{j,n_1})$ from α small matrices, data that can be reused for a matrix of any order).

By the notation of the theory of Generalized Locally Toeplitz (GLT) sequences, see [14] and references therein, we say that f describes the eigenvalue distribution of a matrix A_n , when

$$\{A_n\}_n \sim_{\text{GLT}, \sigma, \lambda} f.$$

Here we do not report the formal definitions for which we refer to [14], but instead we remind that $\{A_n\}_n \sim_{\sigma,\lambda} f$ has the informal meaning that the bulk of singular values, eigenvalues behave, for n large enough and up to infinitesimal errors in the parameter n , as an equispaced sampling of the functions f , $|f|$, respectively over the common definition domain.

In this paper we consider the following types of matrices A_n ,

$$\begin{aligned} A_n &= T_n(f), \\ A_n &= T_n(f) + R_n, \\ A_n &= T_n^{-1}(b)T_n(a), \quad f = a/b, \end{aligned}$$

where f is assumed to be real-valued, continuous and monotone, R_n is a low-rank matrix, and a, b are real-valued cosine polynomials, with b non-negative and not identically zero. We thus have the following more general notation

$$\tilde{\lambda}_j^{(\theta,\alpha)}(A_n) = f(\theta_{j,n}) + \sum_{k=1}^{\alpha} \tilde{c}_k(\theta_{j,n})h^k, \quad (5)$$

$$\tilde{E}_{j,n,\alpha}^{\lambda,\theta} = \lambda_j(A_n) - \tilde{\lambda}_j^{(\alpha)}(A_n). \quad (6)$$

2 Main Results

In this paper we now introduce the “perfect” grid $\xi_{j,n}$, associated with the symbol f and matrix A_n , such that

$$\lambda_j(A_n) = f(\xi_{j,n}), \quad (7)$$

that is, sampling the symbol $f(\theta)$ with $\xi_{j,n}$ gives the exact eigenvalues of A_n . Such a grid has to exist thanks to the continuity of f and thanks to the distributional/localization results (see [8] and references therein). We thus have

$$\xi_{j,n} = \theta_{j,n} + E_{j,n}^{\xi}, \quad (8)$$

where $E_{j,n}^{\xi}$ is error in the sampling grid, using the standard grid (2) instead of the perfect grid $\xi_{j,n}$. We now introduce the following fact, and dedicate the rest of this paper to show applications of this assumption to a number of different Toeplitz-like matrices and their symbols, describing the eigenvalue distribution. Fact 1 follows from (3) and from the monotonicity of f via a proper Taylor expansion.

Fact 1. *There exists an expansion*

$$\xi_{j,n} = \theta_{j,n} + \sum_{k=1}^{\alpha} d_k(\theta_{j,n})h^k + E_{j,n,\alpha}^{\xi}, \quad (9)$$

where $h = 1/(n+1)$, such that we can asymptotically describe a perfect grid $\xi_{j,n}$ such that (7) is true. Of course the latter holds for the same types of symbols for which the expansion (3) has been shown to work for; see for example [2, 10, 12].

We now first present two illustrative examples, and then propose Algorithm 1, a matrix-less method for approximating the functions $d_k(\theta)$ in (9). Finally Algorithm 2 describes how to use the information from Algorithm 1 to approximate the eigenvalues $\lambda_j(A_n)$ for any n . Henceforth we use the following notation

$$\tilde{\xi}_{j,n}^{(\alpha)} = \theta_{j,n} + \sum_{k=1}^{\alpha} \tilde{d}_k(\theta_{j,n})h^k, \quad (10)$$

$$\tilde{E}_{j,n,\alpha}^{\xi} = \xi_{j,n} - \tilde{\xi}_{j,n}^{(\alpha)}, \quad (11)$$

$$\tilde{\lambda}_j^{(\xi,\alpha)}(A_n) = f(\tilde{\xi}_{j,n}^{(\alpha)}), \quad (12)$$

$$\tilde{E}_{j,n,\alpha}^{\lambda,\xi} = \lambda_j(A_n) - \tilde{\lambda}_j^{(\xi,\alpha)}(A_n), \quad (13)$$

to distinguish from the expansion and errors defined in (5) and (6).

Example 1. *In this example we study the symbol $f(\theta) = (2 - 2\cos(\theta))^2 = 6 - 8\cos(\theta) + 2\cos(2\theta)$, associated with the second order finite difference discretization of the bi-Laplacian. It is well known that an equispaced grid does not give the exact eigenvalues of the generated matrices $T_n(f)$ for finite matrices, for example, see discussions in [3, 13].*

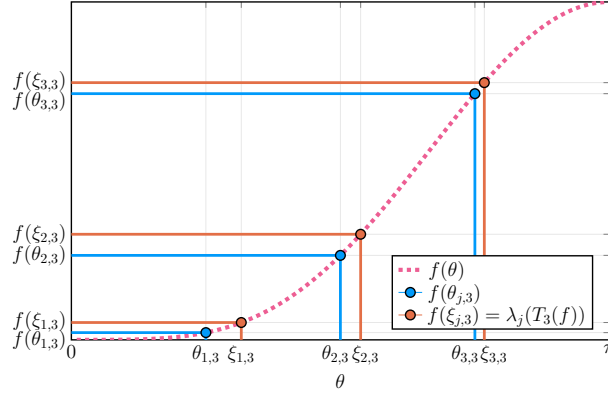


Figure 2: Example 1: Symbol $f(\theta) = (2 - 2 \cos(\theta))^2$ (dashed pink line) and the two expansions approximate the errors $E_{j,n}^{\lambda,\theta} = \lambda_j(T_n(f)) - f(\theta_{j,n}) = f(\xi_{j,n}) - f(\theta_{j,n})$ and $E_{j,n}^\xi = \xi_{j,n} - \theta_{j,n}$.

In Figure 2 we show the symbol f (dashed pink line), and present data for the generated Toeplitz matrix of order $n = 3$, $T_3(f)$, that is, the three eigenvalues $\lambda_j(T_3(f)) = f(\xi_{j,3})$ (red circles) and the three samplings $f(\theta_{j,3})$ (blue circles) where the sampling grid $\theta_{j,3}$ is defined in (2).

Hence, in previous papers, we approximate $E_{j,n}^{\lambda,\theta}$ in (1), by computing the $\tilde{\lambda}_j^{(\theta,\alpha)}(A_n) - f(\theta_{j,n})$ in (5). We thus approximate the error of the eigenvalue approximations when only using the symbol approximation $f(\theta_{j,n})$. The sought error $E_{j,3}^{\lambda,\theta} = \lambda_j(T_3(f)) - f(\theta_{j,3})$ is the distance between the red and blue line on the y-axis.

In this paper we instead study the error $E_{j,n}^\xi$ in (8), by computing the $\tilde{\xi}_{j,n}^{(\alpha)} - \theta_{j,n}$ in (10). Hence, we approximate the error of the grid, when using the standard grid (2). The sought error $E_{j,3}^\xi = \xi_{j,3} - \theta_{j,3}$ is the distance between the red and blue line on the x-axis. Subsequently we can use the approximated $\tilde{\xi}_{j,n}^{(\alpha)}$, in (10), to approximate the eigenvalues $\lambda_j(T_n(f))$ by using (12).

In the following Example 2 we show the first numerical evidence supporting Fact 1.

Example 2. We return to the symbol $f(\theta) = (2 - 2 \cos(\theta))^2$ of Example 1. In Figure 3 we present in the left panel the errors $E_{j,n}^\xi = E_{j,n,0}^\xi$ in (9), for a number of different n , that is,

$$\xi_{j,n} = \cos^{-1} \left(\frac{2 - \sqrt{\lambda_j(T_n(f))}}{2} \right),$$

$$E_{j,n}^\xi = \xi_{j,n} - \theta_{j,n}.$$

The sizes of the matrices, used to compute E_{j,n_k}^ξ are $n_k = 2^{k-1}(n_1 + 1) - 1$, where $n_1 = 100$, and $k = 1, \dots, 4$. In the right panel we have scaled all the errors by $h_k = 1/(n_k + 1)$. The overlap is very good for the curves for different n_k , indicating the general shape of $d_1(\theta)$ in (9), later observed in Figure 5.

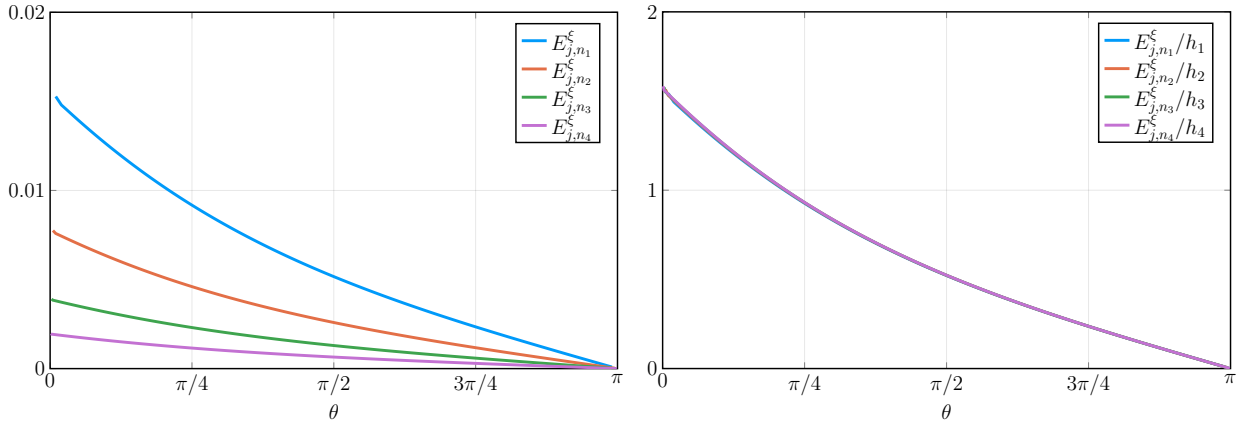


Figure 3: Example 2: Errors ($E_{j,n}^\xi = \xi_{j,n} - \theta_{j,n}$) and scaled errors ($E_{j,n}^\xi/h$). Left: Errors E_{j,n_k}^ξ , for $n_k = 2^{k-1}(n_1 + 1) - 1$, $n_1 = 100$, and $k = 1, \dots, 4$. Right: Scaled errors $E_{j,n_k}^\xi/h_k$ where $h_k = 1/(n_k + 1)$.

Remark 1. For more complicated symbols f , the roots of $f(\theta) - \lambda_j(A_n)$ are $\xi_{j,n}$, and can be computed numerically.

We propose in Algorithm 1 a procedure for approximating $d_k(\theta)$ with $\tilde{d}_k(\theta_{j,n_1})$, for $k = 1, \dots, \alpha$ on the grid points θ_{j,n_1} , defined in (2). In Algorithm 2 we then use the interpolation–extrapolation scheme described in [11] to approximate $d_k(\theta_{j,n})$ for any n , and subsequently use this data to approximate the eigenvalues $\lambda_j A_n$. We here note that a similar approach was developed independently in [1].

Algorithm 1. Approximate the expansion functions $d_k(\theta)$ in (9) in the points θ_{j,n_1} defined in (2).

1. Choose n_1 and α .

2. For each $k = 1, \dots, \alpha$

(a) Compute eigenvalues $\lambda_j(A_{n_k})$ where, for example,

- $A_{n_k} = T_{n_k}(f)$,
- $A_{n_k} = T_{n_k}(f) + R_{n_k} + N_{n_k}$,
- $A_{n_k} = (T_{n_k}(b))^{-1}T_{n_k}(a)$, $f = a/b$,

and $n_k = 2^{k-1}(n_1+1)-1$, R_n is a low-rank matrix and N_n is a small-norm matrix, a, b are real-valued cosine polynomials, with b non-negative and not identically zero; see [14];

(b) Define the indices $j_k = 2^{k-1}j_1$, where $j_1 = \{1, \dots, n_1\}$;

(c) Compute the grid that gives the exact eigenvalues by finding the roots ξ_{j_k, n_k} such that

$$f(\xi_{j_k, n_k}) - \lambda_{j_k}(A_{n_k}) = 0;$$

(d) Store the errors in a matrix $(\mathbf{E})_{k, j_k} = \xi_{j_k, n_k} - \theta_{j_1, n_1}$;

3. Create the Vandermonde matrix $(\mathbf{V})_{i, j} = h_i^j$, where $h_i = 1/(n_i + 1)$, where $i, j = 1, \dots, \alpha$;

4. Compute the \mathbf{D} matrix by solving $\mathbf{V}\mathbf{D} = \mathbf{E}$, that is, $\mathbf{D} = \mathbf{V} \backslash \mathbf{E}$.

Once we have our \mathbf{D} matrix, where $\tilde{d}_k(\theta_{j,n_1}) = (\mathbf{D})_{k, j_1}$, we can utilize them to reconstruct approximately the “perfect” grid $\xi_{j,n}$ for any n . Hence, for an arbitrary n , the full spectrum om A_n is then approximated by (12), by first using a modified version of the interpolation–extrapolation scheme of [11], to get $\tilde{d}_k(\theta_{j,n})$. The procedure is described in Algorithm 2.

Algorithm 2. Compute approximation $\tilde{d}_k(\theta_{j,n})$ from $\tilde{d}_k(\theta_{j,n_1})$, and approximate $\lambda_j(A_n)$.

1. Interpolate–extrapolate $\tilde{d}_k(\theta_{j,n_1})$ to $\tilde{d}_k(\theta_{j,n})$ as is done for $\tilde{c}_k(\theta_{j,n_1})$ in [11];

2. Compute $\tilde{\xi}_{j,n}^{(\alpha)} = \theta_{j,n} + \sum_{k=1}^{\alpha} \tilde{d}_k(\theta_{j,n})h^k$, where $h = 1/(n+1)$;

3. Compute the eigenvalue approximations $\tilde{\lambda}_j^{(\xi, \alpha)}(A_n) = f(\tilde{\xi}_{j,n}^{(\alpha)})$.

3 Numerical Experiments

In this section we consider three different examples, numerically supporting Fact 1. In Example 3 we study the Toeplitz matrix associated with the second order finite difference discretization of the Laplacian, with imposed Neumann–Dirichlet boundary conditions. We examine in Example 4 the grid expansion (10) for the Toeplitz matrix associated with second order finite difference discretization of the bi-Laplacian. Finally the grid expansion (10) for a preconditioned matrix is presented in Example 5.

Example 3. We here study the symbol $f(\theta) = 2 - 2\cos(\theta)$, and the perturbed generated matrix $A_n = T_n(f) + R_n$ of the form

$$A_n = T_n(f) + R_n = \begin{bmatrix} 2 & -1 & & & \\ -1 & 2 & -1 & & \\ & \ddots & \ddots & \ddots & \\ & & \ddots & \ddots & -1 \\ & & & -1 & 2 \end{bmatrix} + \begin{bmatrix} -1 & & & & \\ & & & & \\ & & & & \\ & & & & \\ & & & & \end{bmatrix} = \begin{bmatrix} 1 & -1 & & & \\ -1 & 2 & -1 & & \\ & \ddots & \ddots & \ddots & \\ & & \ddots & \ddots & -1 \\ & & & -1 & 2 \end{bmatrix}.$$

This matrix corresponds to the normalized discretization of second order finite differences and the second derivative operator (Laplacian), with imposed mixed Neumann–Dirichlet boundary conditions. It is known that the eigenvalues of A_n are exactly expressed by

$$\lambda_j(A_n) = f(\xi_{j,n}), \quad \xi_{j,n} = \frac{(j-1/2)\pi}{n+1/2}, \quad j = 1, \dots, n.$$

We thus have

$$E_{j,n}^\xi = \xi_{j,n} - \theta_{j,n} = \frac{(j-1/2)\pi}{n+1/2} - \frac{j\pi}{n+1} = \frac{1}{2n+1} (\theta_{j,n} - \pi),$$

and then

$$E_{j,n}^\xi = \sum_{k=1}^{\infty} d_k(\theta_{j,n}) h^k, \quad h = 1/(n+1),$$

where

$$d_k(\theta_{j,n}) = \frac{1}{2^k} (\theta_{j,n} - \pi).$$

In Figure 4 we present $\tilde{d}_k(\theta_{j,n_1})$, computed with Algorithm 1, and $d_k(\theta_{j,n_1})$ for $k = 1, \dots, \alpha$, for $n_1 = 100, \alpha = 4$. The overlaps of the numerical and theoretical function values are good.

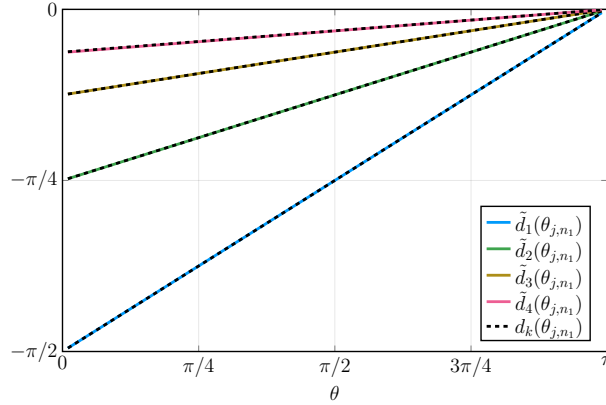


Figure 4: Example 3: Expansion of the grid ξ_{j,n_1} associated with the matrix $A_{n_1} = T_{n_1}(f) + R_{n_1}$, where $f(\theta) = 2 - 2\cos(\theta)$ and R_n is a small rank perturbation (coming from a Neumann boundary condition). The functions $d_k(\theta)$ are well approximated by $\tilde{d}_k(\theta)$.

Example 4. In this example we return to the symbol f discussed in Examples 1 and 2, namely,

$$f(\theta) = (2 - 2\cos(\theta))^2 = 6 - 8\cos(\theta) + 2\cos(2\theta),$$

and employ Algorithms 1 and 2 and study the results.

In Figure 5 we show the computed expansion functions $\tilde{d}_k(\theta_{j,n_1})$, for $n_1 = 100$ and $\alpha = 2$ (left panel) and $\alpha = 3$ (right panel). We note that for example $\tilde{d}_2(\theta_{1,n_1})$ and $\tilde{d}_2(\theta_{2,n_1})$ (red line, closest to $\theta = 0$) is different in the two panels. Also $\tilde{d}_3(\theta_{j,n_1})$ behaves erratic a few approximations close to $\theta = 0$. This effect is due to the fact that the symbol f violates the simple-loop conditions, discussed in detail in [3] and also in [13]. However, this has low impact in the current numerical setting, and also we employ a modification of the extrapolation in [11] by simply ignoring user specified indices for the different $k = 1, \dots, \alpha$.

In the left panel of Figure 6 we show the interpolation–extrapolated $\tilde{d}_k(\theta_{j,n})$ (dashed black lines) for $n_1 = 100, \alpha = 3$, and $n = 100000$. The following samplings were ignored in these computations: for $\tilde{d}_2(\theta_{j,n_1})$ indices $j = 1, 2$ and for $\tilde{d}_3(\theta_{j,n_1})$ indices $j = 1, 2, 3$. In the right panel of Figure 6 is presented the absolute error $\log_{10} |E_{j,n}^\xi|$ of (8) and the subsequent errors $\log_{10} |\tilde{E}_{j,n,\beta}^\xi|$ of (11) for $\beta = 1, 2, 3$. The perfect grid $\xi_{j,n}$ is very well approximated, with a slight reduction of accuracy close to $\theta = 0$. The parameters used for the computations in the right panel of Figure 6 (and also both panels of Figure 7) are $n_1 = 1000, \alpha = 3$, and $n = 100000$. As expected the correction $\tilde{d}_3(\theta_{j,n})h^3$ to $\tilde{E}_{j,n,2}^\xi$ (to get $\tilde{E}_{j,n,3}^\xi$) has only negligible effect since $h^3 = \mathcal{O}(10^{-15})$. Only every 50th (every 100th for $\tilde{E}_{j,n,3}^\xi$) error is plotted for improved clarity in the visualizations. In Figure 7 we

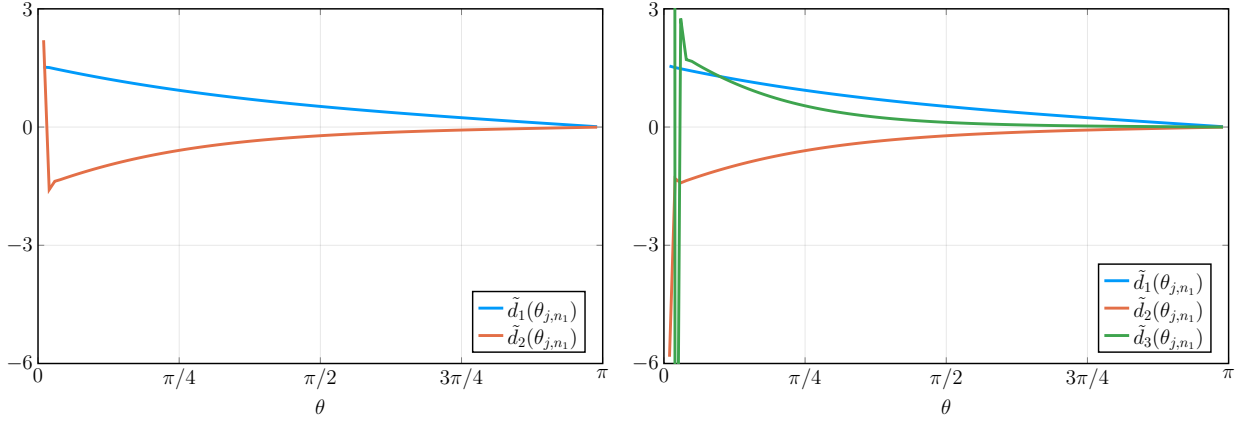


Figure 5: Example 4: Computed expansion function approximations $\tilde{d}_k(\theta_{j,n_1})$, $k = 1, \dots, \alpha$ for $\alpha = 2$ (left) and $\alpha = 3$ (right), and $n_1 = 100$. Note the erratic behavior for $\tilde{d}_2(\theta_{j,n_1})$ and $\tilde{d}_3(\theta_{j,n_1})$ close to $\theta = 0$.

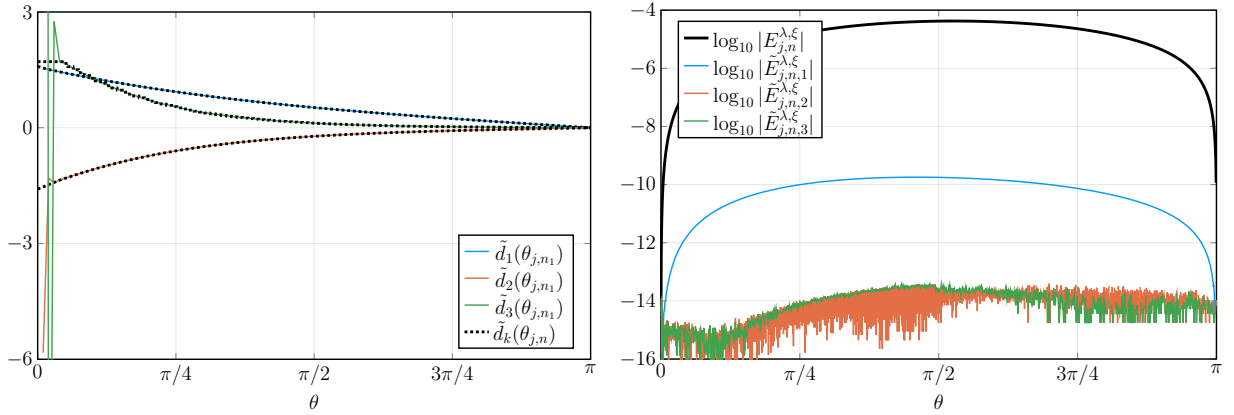


Figure 6: Example 4: Application of Algorithms 1 and 2,. Left: Approximations $\tilde{d}_k(\theta_{j,n_1})$ from Algorithm 1 (colored lines) and $\tilde{d}_k(\theta_{j,n})$ from step 1 of of Algorithm 2 (dashed black lines). Right: The error $E_{j,n}^\xi$ (and $\tilde{E}_{j,n,\beta}^\xi$, for $\beta = 1, 2, 3$).

present the the errors $E_{j,n}^{\lambda,\theta}$ and $E_{j,n}^{\lambda,\xi}$ (and $\tilde{E}_{j,n,\beta}^{\lambda,\theta}$ and $\tilde{E}_{j,n,\beta}^{\lambda,\xi}$ for $\beta = 1, 2, 3$) defined in (1) and (8) (and (6) and (13)). Thus, in the left panel of Figure 7 we show how well $\lambda_j(T_n(f))$ are approximated using the method in [11] (with the addition of removal of erratic points in the interpolation–extrapolation stage). In the right panel of Figure 7 we present how well $\lambda_j(T_n(f))$ are approximated using Algorithms 1 and 2 in this paper. We note that the result in the right panel is better overall for the whole spectrum, but especially close to $\theta = 0$, and machine precision accuracy has almost been achieved.

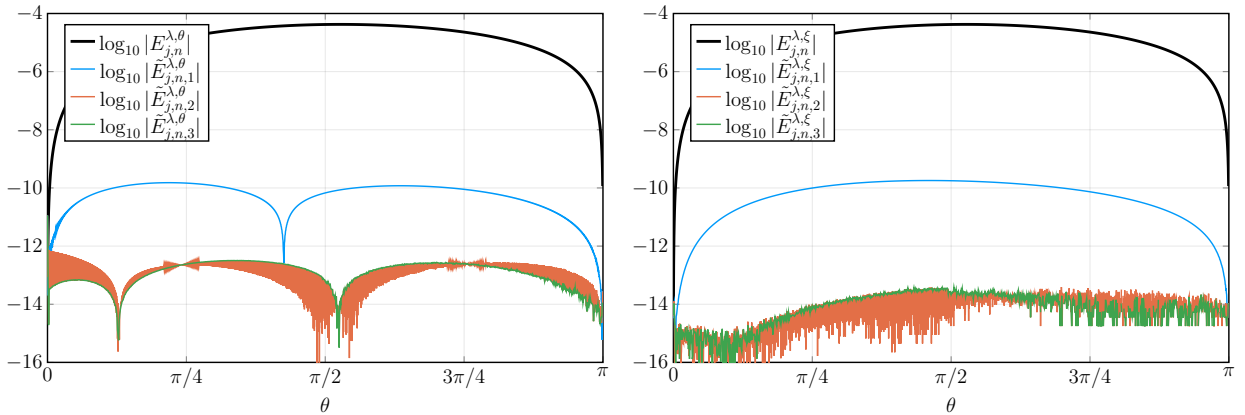


Figure 7: Example 4: Errors of eigenvalue approximations. Left: Errors $\log_{10} |E_{j,n}^{\lambda,\theta}|$ (and $\log_{10} |\tilde{E}_{j,n,\beta}^{\lambda,\theta}|$, for $\beta = 1, 2, 3$). Computations using [11]. Right: Errors $\log_{10} |E_{j,n}^{\lambda,\xi}|$ (and $\log_{10} |\tilde{E}_{j,n,\beta}^{\lambda,\xi}|$, for $\beta = 1, 2, 3$). Computations using Algorithms 1 and 2. Note the overall lower error compared with the left panel, especially close to $\theta = 0$.

Example 5. Preconditioned matrices are important in many applications, and the study of their behavior is hence of importance. We here look at the matrix

$$A_n = T_n^{-1}(a)T_n(b),$$

$$\{A_n\} \sim_{\text{GLT}, \sigma, \lambda} f,$$

where

$$a(\theta) = 4 - 2 \cos(\theta) - 2 \cos(2\theta) = (2 - 2 \cos(\theta))(3 + 2 \cos(\theta)),$$

$$b(\theta) = 3 + 2 \cos(\theta),$$

$$f(\theta) = a(\theta)/b(\theta) = 2 - 2 \cos(\theta),$$

which is Example 1 from [2].

In the left panel of Figure 8 we show the symbols a, b , and $f = a/b$. In the right panel of Figure 8 is shown the absolute error when approximating $\xi_{j,n}$, that is, $\log_{10} |E_{j,n}^\xi|$ (and $\log_{10} |\tilde{E}_{j,n,\beta}^\xi|$ for $\beta = 1, 2, 3$). Like in the right panel of Figure 6 we note a slight reduction of accuracy close to $\theta = 0$, but here also close to $\theta = \pi$.

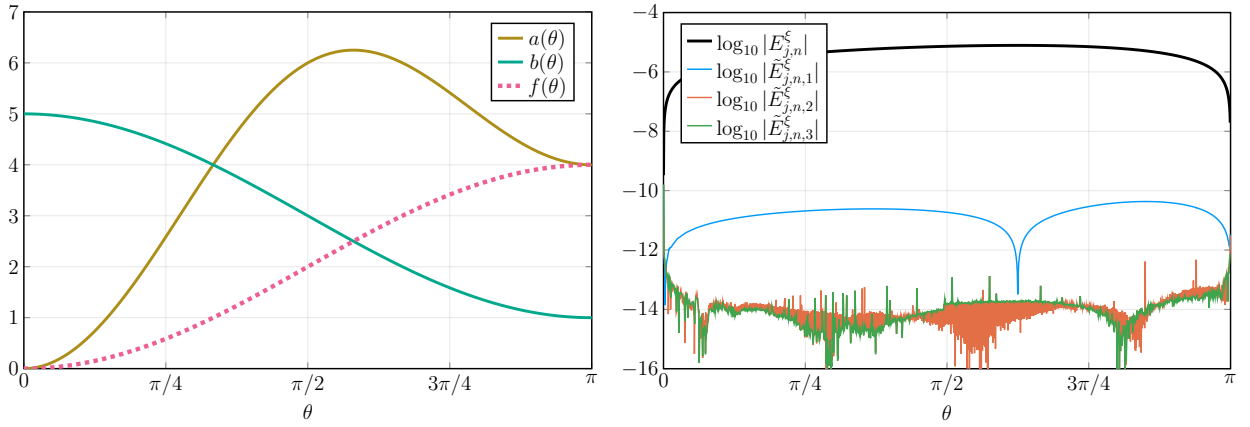


Figure 8: Example 5: Symbols and errors approximating $\xi_{j,n}$. Left: Symbols a, b , and $f = a/b$. Right: $\log_{10} |E_{j,n}^\xi|$ (and $\log_{10} |\tilde{E}_{j,n,\beta}^\xi|$ for $\beta = 1, 2, 3$ for $n_1 = 1000, \alpha = 3$, and $n = 100000$).

In Figure 9 we present both the computed expansion function $\tilde{c}_k(\theta_{j,n})$ (left) and $\tilde{d}_k(\theta_{j,n})$ (right). We note the similarity between the two expansions. Finally in Figure 10 we present the absolute errors when approxi-

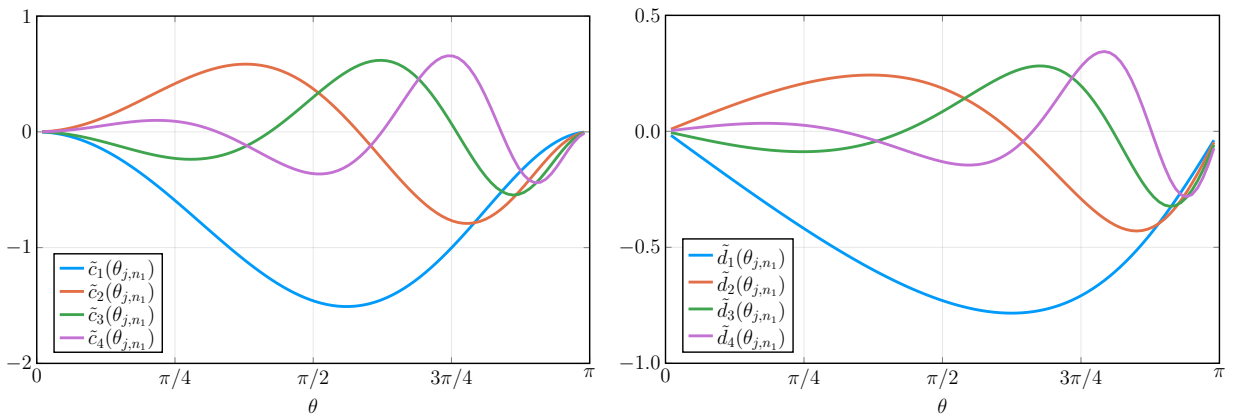


Figure 9: Example 5: Expansions for preconditioned matrix, $n_1 = 100$ and $\alpha = 4$. Left: Expansion $\tilde{c}_k(\theta_{j,n_1})$, for $k = 1, \dots, \alpha$. Right: Expansion $\tilde{d}_k(\theta_{j,n_1})$, for $k = 1, \dots, 4$.

mating $\lambda_j(T_n^{-1}(b)T_n(a))$, that is, $\log_{10} |E_{j,n}^{\lambda,\theta}|$ (left panel) and $\log_{10} |E_{j,n}^{\lambda,\xi}|$ (right panel) (and $\log_{10} |\tilde{E}_{j,n,\beta}^{\lambda,\theta}|$ and $\log_{10} |\tilde{E}_{j,n,\beta}^{\lambda,\xi}|$ for $\beta = 1, 2, 3$). As is noted in Figure 7, the Algorithms 1 and 2 generally perform better than the algorithm in [11]. The additional cost for Algorithms 1 and 2, compared with [11], is negligible. It consists only of finding the αn_1 roots to $f(\theta) - \lambda_{j_k}(A_{n_k})$, for $k = 1, \dots, \alpha$.

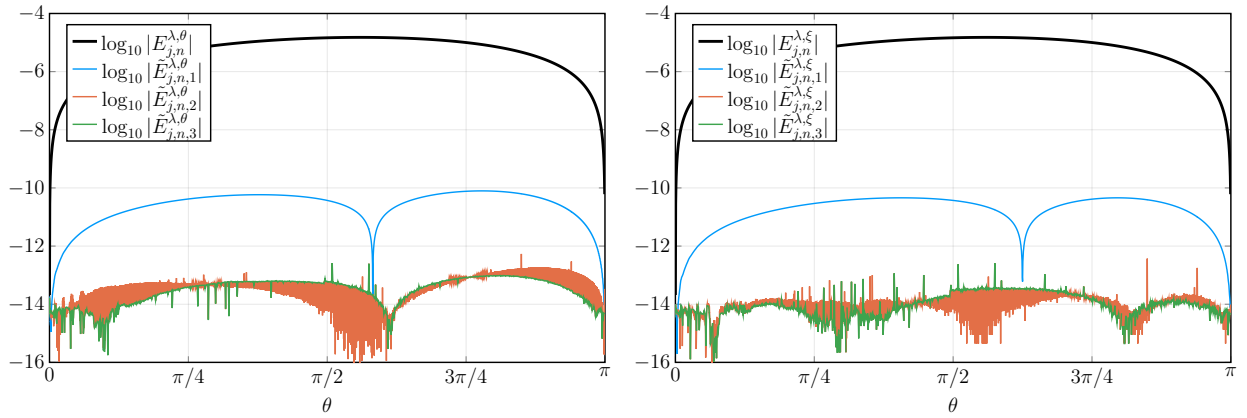


Figure 10: Example 5: Errors of eigenvalue approximations. Left: Errors $\log_{10} |E_{j,n}^{\lambda,\theta}|$ (and $\log_{10} |\tilde{E}_{j,n,\beta}^{\lambda,\theta}|$, for $\beta = 1, 2, 3$). Computations using [11]. Right: Errors $\log_{10} |E_{j,n}^{\lambda,\xi}|$ (and $\log_{10} |\tilde{E}_{j,n,\beta}^{\lambda,\xi}|$, for $\beta = 1, 2, 3$). Computations using Algorithms 1 and 2. Note the overall lower error compared with the left panel.

4 Conclusions

In this paper we have studied the expansion of the grid error $E_{j,n}^{\xi}$ in $\xi_{j,n} = \theta_{j,n} + E_{j,n}^{\xi}$, where $\xi_{j,n}$ is the “perfect” grid associated with a sequence of matrices $\{A_n\}_n$, in the sense that $\lambda_j(A_n) = f(\xi_{j,n})$. Here f is the symbol such that $\{A_n\}_n \sim_{\text{GLT}, \sigma, \lambda} f$. We present an Algorithm 1 to approximate the expansion, proposed in Fact 1, of the error $E_{j,n}^{\xi}$ in (9). In Algorithm 2 we show how to interpolate–extrapolate the data from Algorithm 1, and use this information to approximate the eigenvalues of A_n for arbitrary n . By the numerical experiments in Section 3 we have shown evidence of Fact 1, in a number of practical examples, by also emphasizing the superiority of the new matrix-less method seen in Examples 4 and 5 when approximating the eigenvalues of a large matrix A_n .

The further study of the proposed expansion is warranted, since it might lead to new discoveries on the spectral behavior by applying perturbations of Toeplitz-like matrices, and also faster and more accurate methods to approximate the spectrum of Toeplitz-like matrices. For matrices generated by partially non-monotone symbols we expect similar behavior as for the expansion of the eigenvalue errors: in particular the conclusion is that we can not in general gain any information in the non-monotone part. The block and multilevel cases are also to be considered in future research.

5 Acknowledgments

The author would like to thank Stefano Serra-Capizzano for valuable discussions and suggestions during the preparation of this work. The author is financed by Athens University of Economics and Business.

References

- [1] F. AHMAD, *Equations and Systems of Nonlinear Equations: from high order Numerical Methods to fast Eigensolvers for Structured Matrices and Applications*, PhD thesis, University of Insubria, 2018.
- [2] F. AHMAD, E. S. AL-AIDAROUS, D. A. ALREHAILI, S.-E. EKSTRÖM, I. FURCI, AND S. SERRA-CAPIZZANO, *Are the eigenvalues of preconditioned banded symmetric Toeplitz matrices known in almost closed form?*, Numerical Algorithms, 78 (2017), pp. 867–893.
- [3] M. BARRERA, A. BÖTTCHER, S. M. GRUDSKY, AND E. A. MAXIMENKO, *Eigenvalues of even very nice Toeplitz matrices can be unexpectedly erratic*, in The Diversity and Beauty of Applied Operator Theory, Springer International Publishing, 2018, pp. 51–77.
- [4] J. BOGOYA, A. BÖTTCHER, S. GRUDSKY, AND E. MAXIMENKO, *Eigenvalues of Hermitian Toeplitz matrices with smooth simple-loop symbols*, Journal of Mathematical Analysis and Applications, 422 (2015), pp. 1308–1334.
- [5] J. M. BOGOYA, S. M. GRUDSKY, AND E. A. MAXIMENKO, *Eigenvalues of Hermitian Toeplitz Matrices Generated by Simple-loop Symbols with Relaxed Smoothness*, in Large Truncated Toeplitz Matrices, Toeplitz Operators, and Related Topics, Springer International Publishing, 2017, pp. 179–212.

- [6] A. BÖTTCHER, S. GRUDSKY, AND E. MAKSIMENKO, *Inside the eigenvalues of certain Hermitian Toeplitz band matrices*, Journal of Computational and Applied Mathematics, 233 (2010), pp. 2245–2264.
- [7] A. BÖTTCHER AND B. SILBERMANN, *Introduction to Large Truncated Toeplitz Matrices*, Springer New York, 1999.
- [8] F. DI BENEDETTO, G. FIORENTINO, AND S. SERRA, *C. G. preconditioning for Toeplitz matrices*, Computers & Mathematics with Applications, 25 (1993), pp. 35–45.
- [9] S.-E. EKSTRÖM, I. FURCI, C. GARONI, C. MANNI, S. SERRA-CAPIZZANO, AND H. SPELEERS, *Are the eigenvalues of the B-spline isogeometric analysis approximation of $-\Delta u = \lambda u$ known in almost closed form?*, Numerical Linear Algebra with Applications, 25 (2018), p. e2198.
- [10] S.-E. EKSTRÖM, I. FURCI, AND S. SERRA-CAPIZZANO, *Exact formulae and matrix-less eigensolvers for block banded symmetric Toeplitz matrices*, BIT Numerical Mathematics, 58 (2018), pp. 937–968.
- [11] S.-E. EKSTRÖM AND C. GARONI, *A matrix-less and parallel interpolation–extrapolation algorithm for computing the eigenvalues of preconditioned banded symmetric Toeplitz matrices*, Numerical Algorithms, (2018). <https://doi.org/10.1007/s11075-018-0508-0>, (in press).
- [12] S.-E. EKSTRÖM, C. GARONI, AND S. SERRA-CAPIZZANO, *Are the Eigenvalues of Banded Symmetric Toeplitz Matrices Known in Almost Closed Form?*, Experimental Mathematics, 27 (2018), pp. 478–487.
- [13] S.-E. EKSTRÖM, *Matrix-Less Methods for Computing Eigenvalues of Large Structured Matrices*, PhD thesis, Uppsala University, Uppsala: Acta Universitatis Upsaliensis, 2018.
- [14] C. GARONI AND S. SERRA-CAPIZZANO, *Generalized Locally Toeplitz Sequences: Theory and Applications (Volume 1)*, Springer International Publishing, 2017.